# Loss Analysis of a Rotating Spool Compressor Based on High-Speed Pressure Measurements

International Compressor Engineering Conference at Purdue, July 14-17, 2014

**Craig R. Bradshaw, PhD**
Torad Engineering LLC
Cumming, Georgia

Joe Orosz
Torad Engineering
Cumming, Georgia

Greg Kemp
Torad Engineering LLC
Cumming, Georgia

Eckhard A. Groll, D.Sc.
Ray W. Herrick Laboratories and Cooling Technologies Research Center
West Lafayette, Indiana

# Loss Analysis of Rotating Spool Compressor Based on High-Speed Pressure Measurements

Craig R. BRADSHAW[1*], Greg KEMP[1], Joe OROSZ[1], Eckhard A. GROLL[2]

[1] Torad Engineering
Cumming, GA, USA
(678)366-3399, craig.bradshaw@toradengineering.com

[2] Purdue University, Ray W. Herrick Laboratories,
West Lafayette, IN, USA
(765)494-2140, groll@purdue.edu

* Corresponding Author

## ABSTRACT

A rotating spool compressor is a novel compressor technology that was recently introduced by Kemp et al. (2008). To accelerate the development of the technology, a breakdown of the key losses within the device is presented. The losses include flow losses associated with leakage and over/under compression due to valves and porting. Additionally, frictional losses associated with the key sealing elements and moving components are calculated. All of these losses are combined into Pareto of losses for the spool compressor. This Pareto identifies the dynamic sealing elements as key components to continue development on to achieve the best improvement in efficiency.

## 1. INTRODUCTION

The rotating spool compressor is a novel rotary compressor mechanism most similar to the sliding vane compressor. Primary differences are described by Kemp et al. (2008) and include three key differences from a sliding vane compressor, as shown in Figure 1.

- The vane is constrained by means of an eccentric cam allowing its distal end to be held in very close proximity to the housing bore while never contacting the bore.
- The rotor has affixed endplates that rotate with the central hub and vane forming a rotating spool.
- The use of dynamic sealing elements to minimize leakage between the suction and compression pockets as well as between the process pockets and the compressor containment.

The movement of the rotor is purely rotary with only the vane and tip seals performing any oscillating movement. The eccentric cam will force the movement of the vane to oscillate by twice the eccentricity during a single rotation. The tip seals will oscillate relative to the vane two times per rotation by an amount proportional to the ratio of diameters of the rotor to the housing bore. The tip seal movement amount is roughly an order of magnitude smaller than the eccentricity and follows a sinusoidal path. Analytical details regarding the geometry, including the mathematical expressions describing the chamber volumes, is presented in Bradshaw and Groll (2013).

### 1.1 What differentiates the spool compressor from existing technologies?

A traditional vane machine (either sliding vane or rotary vane) are relatively difficult platforms scale into larger capacity ranges (larger displacement). This problem stems from the interface between the vane and the housing bore and/or the interface between the vane and the end walls of machine. The spool compressor mechanism reduces these problems by constraining the vane at the center of rotation and also rotating the end plate with the vane.

By constraining the vane as close to its center of mass the sliding velocity and kinematic forces are kept at a minimum. In addition, the vane itself is restricted from sliding on the housing bore. Instead, a secondary sealing element, the tip seal, is required to take up the gap between the end of the vane and the housing bore. The tip seal size and weight can

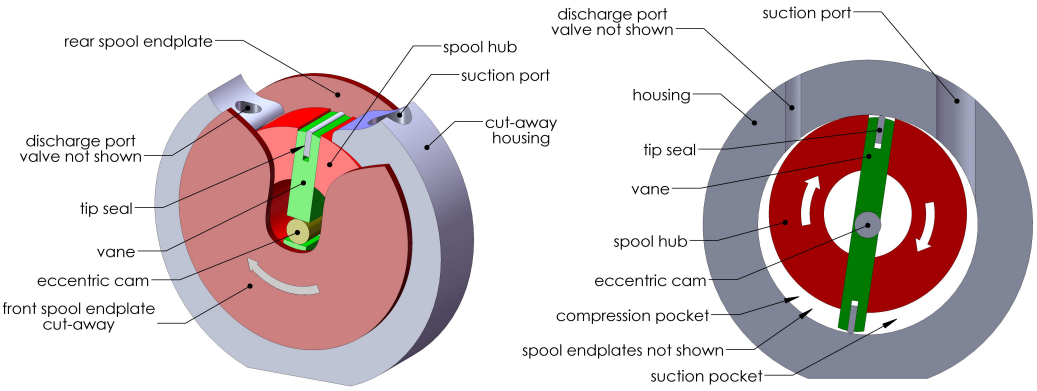


**Figure 1: Cutaway view of rotating spool compressor mechanism with key components highlighted.**

be configured to reduce the frictional losses due to the contact between the housing bore and tip seal. A study of the tip seal design parameters was presented by Bradshaw (2013).

The rotation of the end plates of the spool compressor mechanism greatly reduces the friction generated by the vane. Vane friction not completely eliminated because the vane must slide radially relative to the end plate by an amount equal to the eccentricity. Since the end plate is rotating relative to the compressor housing the gap between these two parts requires sealing. This is accomplished with an additional dynamic sealing element called the spool seal. An overview of the spool seal design constraints has been presented by Kemp et al. (2012). The spool seal can be designed to accommodate various machine applications, such as a seal which can handle a wide operating envelope with adequate sealing. Alternatively, the seal can be designed with lower frictional power loss for applications which have high efficiency demands and a relatively small operating envelope, such as a water-cooled chiller. The rotating end plates can also be utilized for accessory functionality, such as the motive force for a vapor injection valve. Mathison et al. (2013) investigated the tradeoff in the placement and operation of a vapor injection port in the spool compressor. The study found that the spool compressor is relatively insensitive to the placement of an injection port which allows for greater design flexibility.

The combination of these dynamic sealing elements give the spool compressor the flexibility to scale to sizes that have historically proven difficult for other vane technologies. Additionally, this provides flexibility with a specific platform family that is also difficult with traditional vane machines due to the ability to modify the seal designs. In a relatively short amount of time the spool compressor has been able to demonstrate reasonably good performance, as shown by Orosz et al. (2012), compared to conventional technologies which suggest the potential is high.

## 1.2 Dynamic Measurements and Loss Analysis

Dynamic measurements have been historically utilized to examine specific features within compressors. Jacobs (1976) and Dagilis and Vaitkus (2009) utilized indicator diagrams and dynamic pressure measurements in reciprocating compressor to analyze valve dynamics and porting losses. Similarly Lee et al. (2001) performed similar analysis on a linear compressor which allowed for improved valve design. Ng et al. (1980) utilized a similar approach but investigated the valve performance at various operating conditions in an effort to optimize the valve performance over a broad range of operating conditions.

Dynamic measurements have also proved useful in other technologies such as vane compressors. Badr et al. (1985) utilized dynamic measurements to investigate vane chatter and leakage in a multi-vane compressor. Similarly, Jia et al. (2011) investigated the vane dynamics of a multi-vane compressor using high-speed pressure measurements with a variety of vane spring loading. The same studies have proven useful for novel compressor technologies. Kim et al. (2010) utilized dynamic measurements to improve the porting design in the orbiting compressor. These studies can provide a useful method to identify where effort should be focused in initial development. This study will present a tool which can identify all of the key losses within a rotating spool compressor. This is accomplished with a combination of high-speed pressure measurements to identify the flow losses within the mechanism as well as external modeling tools to calculate the frictional load on specific components.

# 2. EXPERIMENTAL METHODS

## 2.1 Sensor Data Collection

A prototype spool compressor is fitted with 3 Endevco 8530B-500 high-speed pressure sensors at locations which will allow a majority of the process pressures to be measured at all rotor angles. The locations are shown in Figure 2 with the angular location of each sensor given in Figure 2b. The only regions which cannot be measured are near the Top Dead Center (TDC) area of the compression process on both the suction and discharge side of the compressor. Since the volume in this region is small it is assumed that any losses or phenomenon that is unable to be measured is also small.

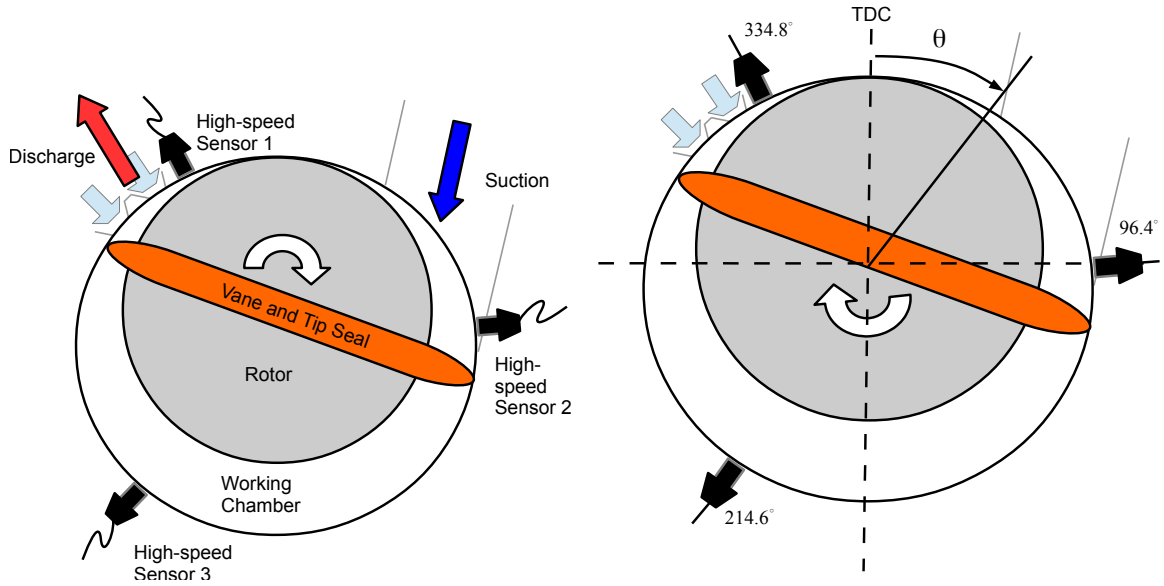


**(a) Sensor locations.** **(b) Angular location of sensors.**

**Figure 2: High-speed sensors within spool compressor geometry.**

The sensors are sampled at 30000 samples per second for all conditions measured. For these tests the operating conditions and fluid are fixed at an air-conditioning load point. Using R410A as the refrigerant the suction pressure is set at 905 kPa (132 psia), discharge pressure of 2282 kPa (331 psia), and 11 K (16 R) of superheat. This corresponds to 4.4 °C (40 °F) and 37.8 °C (100 °F) evaporating and condensing temperatures, respectively. The compressor shaft speed is fixed at 3550 rpm.

Since the location of the pressure sensors is fixed, the instant that the vane passed over the sensor 3, at 214.6 degrees, was used to determine what the pocket volume is at a given instant. Sensor 3 was best suited to this task as this location experienced less pressure fluctuation compared to the other sensors. An algorithm was developed to detect this crossover event, in post processing, and using the geometry model developed by Bradshaw and Groll (2013) this event was correlated to the corresponding chamber volumes. This allows the construction of an experimentally obtained pressure-volume curve, otherwise known as the indicator diagram. Figure 3 is a sample indicator diagram of the spool compressor operating at approximately 3550 rpm. The horizontal dotted lines represent the steady state pressure measurements obtained by pressure sensors in the manifolds external to the compressor. The solid curve in the compression process represents a polytropic compression process which serves as a comparison to ideal.

## 2.2 Experimental Uncertainty

The uncertainty of the loss measurements is represented as a 95% confidence interval calculated using a two-tailed student's t-distribution. The values are an average of 5 samples per operating condition and each sample is 10000 data points. This sample consists roughly 20 cycles which is collected to generate a single cycle sample.

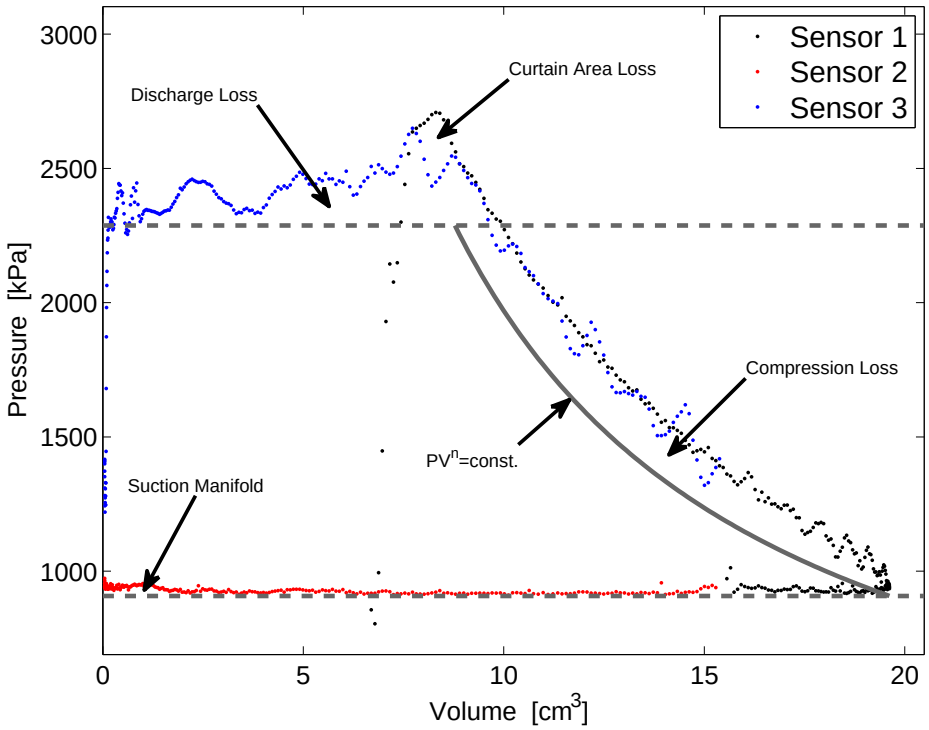


**Figure 3: High speed pressure trace of spool compressor at 3550 rpm.**

## 3. LOSS ANALYSIS

Using the high-speed pressure measurements it was possible to develop a loss Pareto which accounts for a majority of the losses associated with the compressor. The analysis uses a combination of experimentally obtained metrics as well as previously developed modeling tools to estimate the tip seal (Bradshaw (2013)), vane, spool seal, and viscous drag (Bradshaw and Groll (2013)). The remaining losses are assumed to be concentrated in the flow of gas through the compressor. The description of these losses is given in the following sections. Each loss is evaluated by calculating the boundary work relative to nominal for each region.

$$\tau_{loss} = \int P_p dV - \int P_{ideal} dV_{ideal} \tag{1}$$

### 3.1 Discharge

The discharge loss is a result of flow losses associated with the discharge port, valve, and curtain area. Pressure drop associated with these three areas result in a chamber pressure that is higher than the discharge manifold pressure to overcome these losses. This loss is illustrated in Figure 3 and can be calculated using Equation 1 where the chamber pressure is equal to either the compression or discharge chamber during the discharge process depending on the vane location. Since sensor 3 is exposed to the majority of the discharge process Equation 1 can be re-written to express the discharge loss:

$$\tau_{discharge} = \int P_3 dV - P_{dis}(V_{3s} - V_{3e}) \tag{2}$$

where $P_3$ and $dV$ are the pressure and corresponding differential volume at each measurement by sensor 3. $V_{3s}$ is the volume where the first sensor 3 pressure measurement exceeds $P_{dis}$ and $V_{3e}$ is the last measurement where the sensor 3 pressure measurement exceeds $P_{dis}$.

### 3.2 Compression

The compression process losses are associated with pressure during the closed compression process beyond that of an idealized polytropic compression. The polytropic compression is assumed to have a fixed polytropic exponent of 1.11. This value represents the best fit of an adiabatic and reversible compression of a real gas. The loss region is illustrated in Figure 3. This loss contains influence from leakage across the vane, side seal, and tip seals as well as backflow through the discharge valves.

Since sensor 1 is exposed to the entire compression process its measurements are used to calculate the loss associated with the compression process. The calculation is completed in a similar fashion to the discharge process but for convenience completed with respect to pressure:

$$\tau_{compression} = \int V_1 dP - \int \left( \frac{const.}{P_{poly}} \right)^{\frac{1}{n}} dP \tag{3}$$

where $V_1$ is the volume corresponding the with pressure from sensor 1 at each data point.

### 3.3 Suction

Suction losses are associated with flow losses within the suction port as well as leakage that occurs during the suction process. These values are calculated using a similar procedure as the discharge process but requires the addition of the losses associated with both sensors 1 and 2 since neither sensor captures the entire suction process.

### 3.4 Curtain Area

The curtain area of the compressor is shown in Figure 4; it is defined as the area within the compression pocket between the rotor and the edge of the discharge port that is nearest to the suction port. As shown in Figure 4, as the discharge port is moved closer to the suction port the curtain area is increased. Since the curtain area is often of a similar magnitude as the total port area, it is hypothesized that it provides a flow restriction during the discharge process.

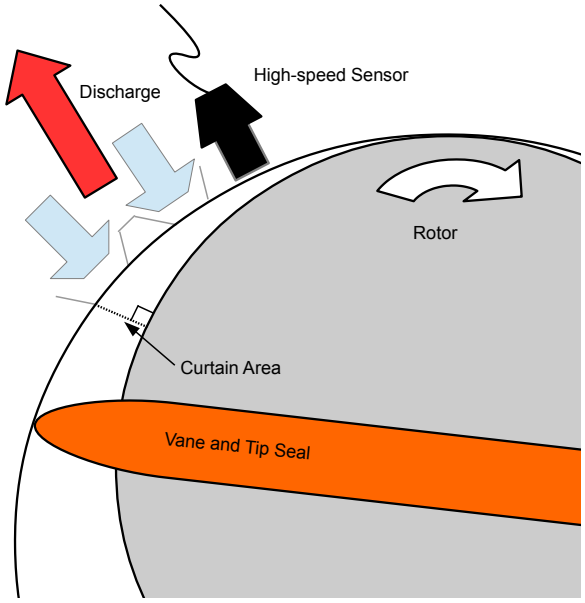


**Figure 4: Example discharge port with curtain area identified in a spool compressor.**

The curtain area loss is associated with the pressure difference between sensors 1 and 3 during the discharge process. This loss is illustrated in Figure 3 during portions of the discharge process. Since sensors 1 and 3 are separated by the curtain area the pressure differential measured between them during the discharge process is assumed to be due to a pressure drop across the curtain area. Therefore the curtain area loss is calculated as follows:

$$\tau_{curtain} = \int P_1 dV - \int P_3 dV \tag{4}$$

where the limits of integration are the volumes where the two sensors are reading the same chamber during the discharge process.

### 3.5 Spool and Tip Seals

The spool seal losses are calculated using a mixed-boundary lubrication model which accounts for both mechanical load support and hydrostatic load support, similar to Lebeck (1988). The tip seal model was previously presented by Bradshaw (2013) where the tip seal was assumed to operate purely hydrodynamic. The hydrodynamic load is balanced against the centrifugal acceleration, pressure load under the seal, and any mechanical loading using springs. These submodels are coupled to the loss analysis and use the basic compressor geometry and operating conditions as inputs to calculate the losses associated with these sealing elements.

### 3.6 Vane and Viscous

The vane friction is estimated using a Newtonian friction model. This model is presented in Bradshaw et al. (2014) as well where the expression describing the friction between the vane and rotor can be written as:

$$\tau_{vane} = \mu N = \mu R_v h_{stator} \left(P_{d,avg} - P_{s,avg}\right)\left(R_s - R_r\right) \tag{5}$$

The viscous loss was determined empirically using a set of prototype hardware without seals or valves. The hardware was connected to warm oil (to maintain similar viscosity to operating conditions) and spun at various speeds with a vacuum pump operating simultaneously on the shell of the compressor. The pressures were measured to ensure no significant differential was experienced. The resulting torque measured at 3550 rpm was approximately 0.56 N-m (5 in-lbf) for this architecture.

## 4. RESULTS

Figure 5 shows the useful output and losses measured on a 5th generation prototype spool compressor. This prototype was found to have a significant amount of of losses associated with the side sealing elements relative to the compression power which suggests that a redesign is necessary provided it does not result in a significant increase in leakage.

The next most significant loss is the compression process losses as measured using the high-speed pressure sensors. These losses suggest that high-pressure gas leaks into the compression pocket during the process. This leakage could potentially come from the spool seals, the wrap-around land, Top-Dead-Center (TDC) gap, or tip seals. It is difficult to determine precisely what influence each potential loss location accounts for in the value presented. However, this value is useful in understanding, generally, how leak-tight the process is.

The viscous losses include losses external to the actual mechanism. This includes bearing and windage losses from the rotating end plates spinning in an oil bath. Additionally, bearing losses are also included in this value.

The vane losses are calculated using the analysis in the previous section but are shown with a high level of uncertainty. This is a reflection of the simplicity of the modeling approach as it is unlikely to capture all of the phenomenon associated with the interaction of the vane and the rotor. The remaining mechanism portion of the losses are associated with the friction in the TDC region, sliding on the eccentric cam, and any oil-shear friction between the endplates and the cylinder block. Given each of these components are certain to be improved as the technology continues to develop though further engineering of materials, clearances, and coatings.

The porting and valve losses represent a combination of pressure drop as a result of discharge port size limitations as well as valve dynamics. Similar to the compression losses, it is difficult to determine the precise difference between the two. However, the dynamics associated with the valve would tend to present with more pressure fluctuations whereas the porting losses would tend to present as more of a fixed pressure drop which tapers to zero at the end of the discharge process. Both phenomenon are observed in Figure 3, therefore it is assumed that additional design effort should be focused on the valve dynamics, port placement, and port size.

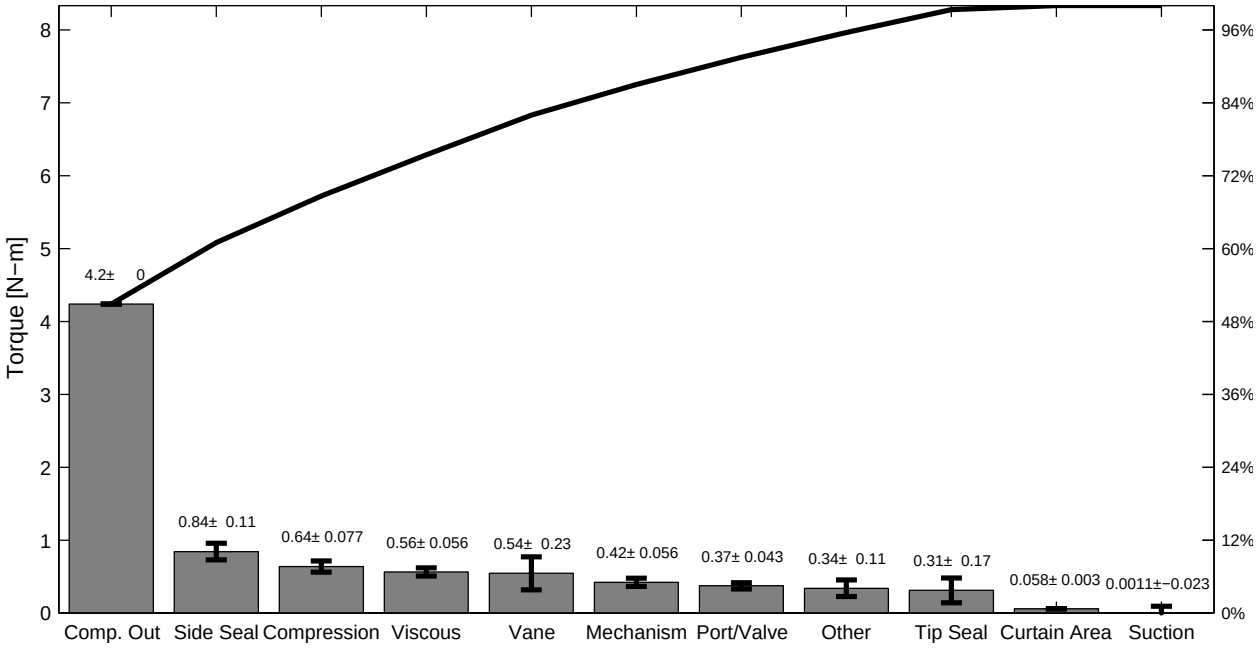


**Figure 5: Loss pareto of a 5th generation spool compressor showing the useful output and key losses estimated from high-speed pressure measurements as well as various friction submodels.**

The tip seal losses are associated with the friction losses of the tip seal riding in the cylinder bore. This component will tend to seal the best when it is in closest proximity to the cylinder bore. However, when the tip seal is in closest proximity to the cylinder bore it will also tend to generate the most frictional load. This tradeoff will need to be investigated with more rigor to maximize the effectiveness of this component.

The curtain area is found to be a small loss, but consistently present. This loss suggests that the port placement is not a critical consideration at this time but may need to be further optimized to achieve maximum effectiveness of this technology. Similarly, the suction losses in the analysis of this particular device are found to be negligible. It is likely this will need to be considered for future prototype platforms but appears sufficient for current prototype purposes.

## 5. CONCLUSIONS

An analysis of the losses within a rotating spool compressor are presented. This loss analysis utilized high-speed pressure measurements to obtain four loss components related to sealing and porting. Additional losses associated with key frictional surfaces are also considered in the analysis. A final pareto of losses in a particular embodiment of the rotating spool compressor is presented. This tool has identified that, in the particular embodiment studied, the side seal, friction and leakage (compression losses), is a key component to improve to increase performance. Additionally, porting and viscous losses should be considered in an updated prototype design.

## NOMENCLATURE

V volume ($cm^3$)
R radius (m)
$h_{stator}$ stator height (m)
P pressure (kPa)
N normal force (N)
**Greek**
$\omega$ rotational speed (rad $sec^{-1}$)

$\mu$ dynamic friction coefficient (-)
$\tau$ loss, torque (N-m)
**Subscript**
stator stator
r rotor
d discharge
s suction
v vane

## REFERENCES

Badr, O., Probert, S., and O'Callaghan, P. (1985). Multi-vane expanders: Internal-leakage losses. *Applied Energy*, 20(1):1--46.

Bradshaw, C. (2013). Spool compressor tip seal design considerations. In *8th International Conference on Compressors and their Systems*, page 341. Elsevier.

Bradshaw, C. R. and Groll, E. A. (2013). A comprehensive model of a novel rotating spool compressor. *International Journal of Refrigeration*, 36(7):1974 -- 1981. New Developments in Compressor Technology.

Bradshaw, C. R., Kemp, G., Orosz, J., and Groll, E. A. (2014). Influence of volumetric displacement and aspect ratio on the performance metrics of the rotating spool compressor. In *International Compressor Engineering Conference at Purdue University*, number 1177.

Dagilis, V. and Vaitkus, L. (2009). Parametric analysis of hermetic refrigeration compressors. *Mechanika*, 6(80):23--29.

Jacobs, J. J. (1976). Analytic and experimental techniques for evaluating compressor performance losses. In *International Compressor Engineering Conference at Purdue University*, number 179.

Jia, X., Zhang, B., Pu, L., Guo, B., and Peng, X. (2011). Improved rotary vane expander for trans-critical co2 cycle by introducing high-pressure gas into the vane slots. *International Journal of Refrigeration*, 34(3):732 -- 741.

Kemp, G., Orosz, J., Bradshaw, C., and Groll, E. A. (2012). Spool seal design and testing for the spool compressor. In *International Compressor Engineering Conference at Purdue University*, number 1259.

Kemp, G. T., Garrett, N., and Groll, E. A. (2008). Novel rotary spool compressor design and preliminary prototype performance. In *International Compressor Engineering Conference at Purdue University*, number 1328.

Kim, H., Kim, W., and Ahn, J. (2010). Orbiting compressor for residential air-conditioners. *International Journal of Refrigeration*, 33:95--106.

Lebeck, A. (1988). Contacting mechanical seal design using a simplified hydrostatic model. *Tribology International*, 21(1):2 -- 14.

Lee, H., Heo, J., Song, G., Park, K., Hyeon, S., and Jeon, Y. (2001). Loss analysis of linear compressor. In *Compressors and their Systems: 7th International Conference*, page 305.

Mathison, M. M., Braun, J. E., and Groll, E. A. (2013). Modeling of a novel spool compressor with multiple vapor refrigerant injection ports. *International Journal of Refrigeration*, 36(7):1982--1997.

Ng, E., Tramschek, A., and MacLaren, J. (1980). Computer simulation of a reciprocating compressor using a real gas equation of state. In *International Compressor Engineering Conference at Purdue University*, number 304.

Orosz, J., Kemp, G., Bradshaw, C., and Groll, E. A. (2012). Performance and operating characteristics of a novel rotating spool compressor. In *International Compressor Engineering Conference at Purdue University*, number 1257.